NUCLEAR SCIENCE AND ENGINEERING

DOI: https://doi.org/10.1080/00295639.2020.1799603

Diffusion Synthetic Acceleration for Heterogeneous Domains, Compatible with Voids

B. S. Southworth,[a]* Milan Holec,[b] and T. S. Haut[b]

[a]*University of Colorado Engineering Center, Department of Applied Mathematics, ECOT 225, 526 UCB, Boulder, Colorado 80309-0526*
[b]*Lawrence Livermore National Laboratory, 7000 East Avenue, Livermore, California 94550*

Received February 3, 2020
Accepted for Publication July 19, 2020

Abstract — *A standard approach to solving the S_N transport equations is to use source iteration with diffusion synthetic acceleration (DSA). Although this approach is widely used and effective on many problems, there remain some practical issues with DSA preconditioning, particularly on highly heterogeneous domains. For large-scale parallel simulation, it is critical that both (a) preconditioned source iteration converges rapidly and (b) the action of the DSA preconditioner can be applied using fast, scalable solvers, such as algebraic multigrid (AMG). For heterogeneous domains, these two interests can be at odds. In particular, there exist DSA diffusion discretizations that can be solved rapidly using AMG, but they do not always yield robust/fast convergence of the larger source iteration. Conversely, there exist robust DSA discretizations where source iteration converges rapidly on difficult heterogeneous problems, but fast parallel solvers like AMG tend to struggle applying the action of such operators. Moreover, very few current methods for the solution of deterministic transport are compatible with voids. This paper develops a new heterogeneous DSA preconditioner based on only preconditioning the optically thick subdomains. The resulting method proves robust on a variety of heterogeneous transport problems, including a linearized hohlraum mesh related to inertial confinement fusion. Moreover, the action of the preconditioner is easily computed using $\mathcal{O}(1)$ AMG iterations, convergence of the transport iteration typically requires 2 to 5× fewer iterations than current state-of-the-art "full" DSA, and the proposed method is trivially compatible with voids. On the hohlraum problem, rapid convergence is obtained by preconditioning less than 3% of the mesh elements with five to ten AMG iterations.*

Keywords — *Transport, discrete ordinates, high order, sweep, unstructured.*

Note — *Some figures may be in color only in the electronic version.*

I. INTRODUCTION

Solving particle transport equations arises in numerous fields of research such as nuclear reactor design, inertial confinement fusion (ICF), and medical imaging. Despite decades of research, however, this remains a computationally expensive and challenging problem. The simplified steady-state, monoenergetic neutral particle transport equation for the spatially and angularly dependent angular flux ψ is given by

$$\begin{aligned}\boldsymbol{\Omega}\cdot\ &\psi(\mathbf{x},\boldsymbol{\Omega})+\sigma_t(\mathbf{x})\psi(\mathbf{x},\boldsymbol{\Omega})\\ &=\frac{\sigma_s(\mathbf{x})}{4\pi}\int_{\mathbb{S}^2}\psi(\mathbf{x},\boldsymbol{\Omega}')d\boldsymbol{\Omega}'+q(\mathbf{x},\boldsymbol{\Omega})\ .\end{aligned}\tag{1}$$

Here, $0\le\sigma_s\le\sigma_t$ are the spatially dependent scattering and total cross sections, respectively, and we assume isotropic scattering for simplicity. This equation is fundamental to

*E-mail: ben.s.southworth@gmail.com

models of neutral particle transport such as neutron or photon transport and is also a prerequisite for solving more complicated physical models such as thermal radiative transfer. The left side of Eq. (1) is a three-dimensional advection-reaction equation in direction $\mathbf{\Omega}$, and the right side is an integral-operator coupling over direction. More complex physical models introduce a nonlinearity in temperature on the right side, while including time and energy leads to seven dimensions, overall requiring massively parallel simulations.

In this paper, we consider an S_N angular discretization of the integral operator in Eq. (1). Using n directions in the angular quadrature set yields the following semi-discrete form of Eq. (1):

$$\begin{aligned} \mathbf{\Omega}_d \cdot \ {}_{\mathbf{x}}\psi_d(\mathbf{x}) + \sigma_t(\mathbf{x})\psi_d(\mathbf{x}) \\ = q_d(\mathbf{x}) + \frac{\sigma_s(\mathbf{x})}{4\pi}\sum_{d\prime=1}^{n}\omega_{d\prime}\psi_{d\prime}(\mathbf{x}), \mathbf{x}\in\mathcal{D}\ , \\ \psi_d(\mathbf{x}) \quad = \psi_{d,inc}(\mathbf{x}), \mathbf{x}\in\partial\mathcal{D} \text{ and } \mathbf{n}(\mathbf{x})\cdot\mathbf{\Omega}_d < 0\ , \end{aligned} \tag{2}$$

where subscript d denotes a fixed angle in the S_N angular discretization, with weight ω_d and direction $\mathbf{\Omega}_d$. Here, $\psi_d(\mathbf{x})$ denotes the angular flux associated with direction d, and the scalar flux is then defined as

$$\varphi(\mathbf{x}) := \sum_{d\prime=1}^{n} w_{d\prime}\psi_{d\prime}(\mathbf{x})\ .$$

Because of the high dimensionality of the transport equations, memory is one of the fundamental constraints in solving them numerically. Fortunately, it is generally the case that $\{\psi_d\}$ can be eliminated from the problem and scalar flux φ can be iterated to convergence thus only requiring storage of one vector on the spatial domain rather than one for each angle. This is discussed formally in a linear algebraic setting in Sec. II.B.

A common approach to solve Eq. (1) is based on a fixed-point iteration where each iteration inverts the left side for each direction in the S_N angular discretization. We will refer to this set of inversions as a transport update, which is the dominant computational cost of solving the transport equations. Upwinded discontinuous discretizations are particularly amenable to an efficient update (and commonly used for this reason) because the linear system for each direction can be solved directly using a forward solve. A transport sweep then consists of a parallel implementation of simultaneous forward solves for all directions in the quadrature set. For $\sigma_t \ll 1$ or $\sigma_s \ll \sigma_t$, fixed-point iteration based on a transport update converges rapidly. For $\sigma_t \approx \sigma_s \gg 1$, the fixed-point operator is very slow to converge but can be effectively preconditioned with so-called diffusion synthetic acceleration (DSA). DSA corresponds to using an appropriate discrete diffusion operator as a preconditioner for the fixed-point iteration on the scalar flux, which is the focus of this paper.

Diffusion synthetic acceleration was developed in separate works in the 1960s as an acceleration technique for solving the transport equations by approximating the behavior of the scalar flux in optically thick materials with a diffusion equation.[1,2] DSA was analyzed and improved for specific discretizations in the 1970s (for example, Ref. 3), and a new scaling of the transport equations was introduced in Ref. 4 to analyze DSA preconditioning. Since then, DSA has seen significant research over the years. Some of the most important general observations include (a) the need for a so-called consistency between the discretization of the linear transport equation and the diffusion preconditioning and (b) the degraded effectiveness of DSA in heterogeneous media.[5] In particular, DSA is known to be effective and easy to apply on homogeneous and optically thick domains, $\sigma_t \gg 1$. However, it is not uncommon for σ_s and σ_t to vary by many orders of magnitude over a spatial domain, and such heterogeneous domains remain difficult for existing methods.

The practical difficulties of DSA on heterogeneous domains come from trying to satisfy both of the following requirements for a fast, parallel transport simulation:

1. The DSA discretization must be an effective preconditioner of the S_N transport equations, resulting in rapid convergence.

2. The DSA preconditioning must be able to be applied in a fast, parallel manner.

In most cases these two goals can be satisfied individually, and for some problems both can be satisfied. However, it is often difficult or impossible to satisfy both using existing techniques on highly heterogeneous domains. Part of this problem comes from the requirement of consistency between the transport and diffusion discretizations. In particular, the transport equations are often discretized using some form of upwind discontinuous discretization. It turns out the compatible DSA preconditioner involves inverting a symmetric interior penalty (SIP) type of diffusion discretization. It is well known though that fast solvers such as algebraic multigrid (AMG) tend to struggle on discontinuous discretizations, even of elliptic problems. This is compounded by the fact that these compatible DSA diffusion discretizations can have very poor conditioning[6] [worse than a standard diffusion conditioning of $\sim\mathcal{O}(1/h^2)$].

Thus, the dichotomy is as follows: Rapid convergence on highly heterogeneous domains requires DSA

based on specific discontinuous diffusion discretizations. However, such discretizations are between difficult and just not amenable to existing fast, parallel linear solvers, such as AMG, particularly if using existing parallel linear solver libraries such as the *hypre* library.[7] A number of works have considered how to construct more effective algebraic solvers for such diffusion discretizations, including in the transport community[8,9] as well as the linear solver community,[10–12] but to our knowledge (and experience testing various methods), heterogeneous problems remain difficult for existing methods, particularly methods that are publicly available and implemented in parallel. Furthermore, it is generally the case that DSA bilinear forms have a diffusion coefficient proportional to $1/\sigma_t(\mathbf{x})$, which is not well-defined if there are any regions of vacuum, $\sigma_t = 0$. Some works have developed appropriate linear and nonlinear DSA modifications when using the self-adjoint angular flux formulation of transport,[13,14] but to our knowledge, DSA applied to the S_N transport equations in domains with voids remains an open question.

This paper derives a new DSA-like preconditioner (not discretization) for heterogeneous domains that is (a) easier to apply in a fast and scalable manner with existing solvers than standard DSA, (b) a better preconditioner than even the most robust standard DSA preconditioners we have tested, and (c) amenable to vacuum. Conceptually, the new algorithm is quite simple and more or less corresponds to only applying DSA preconditioning on "thick" regions in the domain.[a] Using variations in a crooked pipe benchmark problem, the new heterogeneous DSA method reduces the total number of iterations to convergence by 5 to 6× for some problems. Moreover, the heterogeneous DSA matrices are more tractable to solve using AMG, in a number of tests converging in $\mathcal{O}(1)$ iterations when AMG was unable to solve the "full" DSA matrix. The new method is relatively nonintrusive in the sense that it can be added to existing libraries that support DSA with minimal work. Conceptually, the preconditioner is independent of the discretization. However, a discussion on implementation and numerical results are presented based on a discontinuous Galerkin (DG) discretization of the S_N transport equations and corresponding DG DSA discretization.[6,16]

Section II presents standard source iteration and DSA in the context of block preconditioners. This motivates a similar analysis applied specifically to DSA preconditioning, and the development of the new heterogeneous DSA preconditioning in Sec. II.C. An implementation involving the *hypre* library and DG spatial discretizations is discussed in Sec. III, including a generalization of the modified penalty coefficient introduced in Ref. 16 for high-order curvilinear meshes. Numerical results then demonstrate the new method on heterogeneous domains in Sec. IV, including on variations of a crooked pipe problem,[17,18] and a linearized hohlraum capsule. For the hohlraum, in particular, rapid convergence is obtained when applying (heterogeneous) DSA preconditioning to less than 3% of mesh elements! Some conclusions are given in Sec. V.

II. PRECONDITIONING LINEAR TRANSPORT

II.A. Review of 2×2 Block Preconditioners

Source iteration and DSA applied to linear S_N transport can be seen in a linear-algebraic framework as a block preconditioning of a 2×2 block operator. A linear-algebraic perspective on transport iterations was introduced as early as 1989 in Ref. 19,[b] and transport iterations are often expressed in algebraic operator form (for example, see Ref. 16). The specific context of 2×2 block preconditioners is not something seen often in the literature, but it provides valuable insight on the preconditioning of heterogeneous domains.

As a background, consider a 2×2 block matrix A and lower-triangular preconditioner L,

$$A = \begin{bmatrix} A_{11} & A_{12} \\ A_{21} & A_{22} \end{bmatrix}, \quad L = \begin{bmatrix} A_{11} & \mathbf{0} \\ A_{21} & \widehat{\mathcal{S}} \end{bmatrix}, \tag{3}$$

where $\mathcal{S} := A_{22} - A_{21}A_{11}^{-1}A_{12}$ is the Schur complement of A in the $(2,2)$ block and $\widehat{\mathcal{S}}$ is some approximation to $\mathcal{S}$. In the simplest case of a block Gauss-Seidel–like iteration, we have $\widehat{\mathcal{S}} := A_{22}$. It can be shown that fixed-point or Krylov iterations applied to $A\mathbf{x} = \mathbf{b}$ with preconditioner L^{-1} converge to some tolerance $< C\varepsilon$ after k iterations if and only if equivalent iterations applied to a Schur complement problem $\mathcal{S}\mathbf{x}_c = \mathbf{b}_c$, with preconditioner $\widehat{\mathcal{S}}^{-1}$, converge to tolerance ε after k iterations, where $C \sim \mathcal{O}(\| A_{11}^{-1}A_{12} \|)$ (Ref. 20). As it turns out, source iteration and DSA preconditioning correspond exactly to

[a] Recent work in Ref. 15 has seen success applying similar ideas to precondition the radiation diffusion equations by only solving the diffusion discretization on a physical subdomain.

[b] Unfortunately, the only available copy of Ref. 19 appears to be a low-resolution, scanned-in copy, which is difficult to read.

a block lower-triangular preconditioning, as in Eq. (3), and considering transport iterations in the context of block preconditioners allows us to derive a natural approach to DSA preconditioning in heterogeneous media.

II.B. Source Iteration as a Block Preconditioner

Now suppose the left side of Eq. (2) is discretized in space for each direction d, with corresponding discrete spatial operator $\mathcal{L}_d \sim \mathbf{\Omega}_d \cdot \nabla_{\mathbf{x}} + \sigma_t$, and let Σ_s and Σ_t denote mass matrices with respect to coefficients $\sigma_s(\mathbf{x})/4\pi$ and $\sigma_t(\mathbf{x})$, respectively. Further, let bold ψ_d and q_d denote the discrete vector representations of $\psi_d(\mathbf{x})$ and $q_d(\mathbf{x})$. Then, the full discretized set of equations can be written as a block linear system:

$$\begin{bmatrix} \mathcal{L}_1 & & & -\Sigma_s \\ & \ddots & & \vdots \\ & & \mathcal{L}_n & -\Sigma_s \\ -\omega_1 I & & -\omega_n I & I \end{bmatrix} \begin{bmatrix} \psi_1 \\ \vdots \\ \psi_n \\ \varphi \end{bmatrix} = \begin{bmatrix} \mathbf{q}_1 \\ \vdots \\ \mathbf{q}_n \\ \mathbf{0} \end{bmatrix} . \tag{4}$$

The dotted lines indicate how the S_N transport equations can be expressed as a 2×2 block array, Eq. (3): A_{11} is the block-diagonal set of spatial operators $\{\mathcal{L}_d\}$; $A_{22} = I$; and the off-diagonal operators A_{12} and A_{21} correspond to scattering and quadrature weights, respectively.

One of the standard approaches to solve Eq. (4) in transport simulations is to update the scalar flux based on the current angular flux,

$$\psi_d^{(i+1)} = \mathcal{L}_d^{-1}(\mathbf{q}_d + \Sigma_s \varphi^{(i)}) , \tag{5}$$

for all directions $d = 1, ..., n$. With the updated scalar flux for each direction, the angular flux is then updated by summing the scalar flux over quadrature weights $\{\omega_d\}$:

$$\begin{aligned} \varphi^{(i+1)} &= \sum_{d=1}^{n} \omega_d \psi_d^{(i+1)} \\ &= \sum_{d=1}^{n} \omega_d \mathcal{L}_d^{-1} \left(\mathbf{q}_d + \Sigma_s \varphi^{(i)} \right) . \end{aligned} \tag{6}$$

This process is repeated and is the classical source iteration. Algebraically, source iteration is exactly a fixed-point iteration with block lower-triangular preconditioning:

$$\begin{bmatrix} \psi_1^{(i+1)} \\ \vdots \\ \psi_n^{(i+1)} \\ \varphi^{(i+1)} \end{bmatrix} = \begin{bmatrix} \psi_1^{(i)} \\ \vdots \\ \psi_n^{(i)} \\ \varphi^{(i)} \end{bmatrix} + \begin{bmatrix} \mathcal{L}_1 & & & \\ & \ddots & & \\ & & \mathcal{L}_n & \\ -\omega_1 I & & -\omega_n I & I \end{bmatrix}^{-1} \left(\begin{bmatrix} \mathbf{q}_1 \\ \vdots \\ \mathbf{q}_n \\ \mathbf{0} \end{bmatrix} - \begin{bmatrix} \mathcal{L}_1 & & & -\Sigma_s \\ & \ddots & & \vdots \\ & & \mathcal{L}_n & -\Sigma_s \\ -\omega_1 I & & -\omega_n I & I \end{bmatrix} \begin{bmatrix} \psi_1^{(i)} \\ \vdots \\ \psi_n^{(i)} \\ \varphi^{(i)} \end{bmatrix} \right) .$$

Expanding on this, one arrives at exactly the two-stage iteration for $\{\psi_d\}$ and φ introduced in Eqs. (5) and (6). In this form, it is also clear how Krylov methods can be applied to accelerate convergence of source iteration.[5,21] In particular, Krylov methods require computing the action of operator A and preconditioner M^{-1} on vectors, where

$$A = \begin{bmatrix} \mathcal{L}_1 & & & -\Sigma_s \\ & \ddots & & \vdots \\ & & \mathcal{L}_n & -\Sigma_s \\ -\omega_1 I & & -\omega_n I & I \end{bmatrix} ,$$

$$M^{-1} = \begin{bmatrix} \mathcal{L}_1^{-1} & & & \\ & \ddots & & \\ & & \mathcal{L}_n^{-1} & \\ \omega_1 \mathcal{L}_1^{-1} & & \omega_n \mathcal{L}_n^{-1} & I \end{bmatrix} .$$

Note that in source iteration, the transport update inverts $\mathcal{L}_d^{-1}$ for all $d = 1, ..., n$, meaning that in the 2×2 block sense, A_{11} is inverted exactly. Recall from Sec. II.A that convergence of fixed-point or Krylov iterations with a 2×2 block lower-triangular preconditioner is then defined by equivalent iterations on the preconditioned Schur complement problem. In this case, in the notation of Eq. (3), we have $\widehat{\mathcal{S}} = A_{22} = I$, and the preconditioned Schur complement takes the form $\mathcal{S}\varphi = \mathbf{b}$, where

$$\begin{aligned} \mathcal{S} &:= I - \begin{bmatrix} \omega_1 I & & \omega_n I \end{bmatrix} \begin{bmatrix} \mathcal{L}_1^{-1} & & \\ & \ddots & \\ & & \mathcal{L}_n^{-1} \end{bmatrix} \begin{bmatrix} \Sigma_s \\ \vdots \\ \Sigma_s \end{bmatrix} \\ &= I - \sum_{d=1}^{n} \omega_d \mathcal{L}_d^{-1} \Sigma_s \end{aligned} \tag{7}$$

and $\mathbf{b} := \sum_{d=1}^{n} \omega_d \mathcal{L}_d^{-1} \mathbf{q}_d$. If $\mathcal{S}$ is well conditioned, such as in the optically thin case when $\Sigma_s \ll 1$, we can solve $\mathcal{S}\varphi = \mathbf{b}$ via a simple Richardson iteration,

$$\begin{aligned}\varphi^{(i+1)} &= \varphi^{(i)} + \mathbf{b} - \mathcal{S}\varphi^{(i)} \\ &= \sum_{d=1}^{n} \omega_d \mathcal{L}_d^{-1} \left(\mathbf{q}_d + \Sigma_s \varphi^{(i)} \right) . \end{aligned} \tag{8}$$

If $\mathcal{S}$ is ill conditioned, such as in optically thick or heterogeneous media, some form of preconditioner for $\mathcal{S}$ is necessary for fast convergence. In the larger system, this simply replaces I in the lower right $(2,2)$ block of preconditioner M^{-1} with some approximation to $\mathcal{S}$. Denoting this approximation $\mathcal{D}$, the preconditioner takes the form

$$\begin{aligned} M^{-1} &= \begin{bmatrix} \mathcal{L}_1 & & & \\ & \ddots & & \\ & & \mathcal{L}_n & \\ -\omega_1 I & & -\omega_n I & \mathcal{D} \end{bmatrix}^{-1} \\ &= \begin{bmatrix} I & & & \\ & \ddots & & \\ & & I & \\ & & & \mathcal{D}^{-1} \end{bmatrix} \begin{bmatrix} \mathcal{L}_1^{-1} & & & \\ & \ddots & & \\ & & \mathcal{L}_n^{-1} & \\ \omega_1 \mathcal{L}_1^{-1} & & \omega_n \mathcal{L}_n^{-1} & I \end{bmatrix} . \end{aligned} \tag{9}$$

Now, convergence of fixed-point or Krylov iterations applied to the larger system, Eq. (4), is defined by convergence of equivalent iterations applied to $\mathcal{D}^{-1}\mathcal{S}$. In assuming that $\mathcal{L}_d$ is inverted for all d (rather than, say, an on-processor solve), $\{\psi_d\}$ can be eliminated from the system, yielding a preconditioned fixed-point iteration on φ :

$$\begin{aligned}\varphi^{(i+1)} &= \varphi^{(i)} \\ &\quad - \mathcal{D}^{-1} \left(\varphi^{(i)} - \sum_{d=1}^{n} \omega_d \mathcal{L}_d^{-1} \left(\Sigma_s \varphi^{(i)} + \mathbf{q}_d \right) \right) . \end{aligned} \tag{10}$$

At any point, an approximation to the angular flux can be computed via Eq. (5) (and is implicitly computed within every iteration). Similar to the case of source iteration, it is straightforward to analyze and implement Krylov methods here as well, where $\mathcal{S}$ is the operator and $\mathcal{D}^{-1}$ is the preconditioner. It is worth pointing out that for linear S_N transport as considered here, if angular flux $\{\psi_d^{(i+1)}\}$ is eliminated from the system, it is clear that Krylov convergence is defined by convergence on the Schur complement (scalar flux). For nonlinear or time-dependent transport problems, where the angular flux cannot be fully eliminated, this relation is less obvious without considering iterations in the context of 2×2 block preconditioning and appealing to the theory on block preconditioners and Krylov methods.[20]

Note that in practice, $\mathcal{D}$ is not directly a diffusion operator; rather, $\mathcal{D}^{-1} = I + D^{-1}\Sigma$ is an additive preconditioner, with diffusion operator D and mass matrix $\Sigma \sim \sigma_s(\mathbf{x})$ or $\Sigma \sim \sigma_t(\mathbf{x})$.[c] There are various ways to motivate the additive preconditioner. Conceptually, a diffusion operator can be derived in which $D^{-1}\Sigma\mathcal{S}$ is well conditioned in the optically thick limit of mean free path $\varepsilon \ll 1$ (for DG discretizations, see Refs. 6 and 16). However, in optically thin material, $\Sigma_s \ll 1$, $D^{-1}\Sigma\mathcal{S}$ can be ill conditioned because $\mathcal{S}$ is already well conditioned in thin material, but the spectrum of D^{-1} goes to zero for high-frequency modes. Adding the identity shifts such eigenmodes so that $(I + D^{-1}\Sigma)\mathcal{S}$ is well conditioned in thin regimes, while for thick regimes, note that if $D^{-1}\Sigma\mathcal{S}$ is positive and well conditioned, then $(I + D^{-1}\Sigma)\mathcal{S}$ is also positive and well conditioned.

Remark 1: If $\mathcal{L}_d$ is not inverted exactly due to, for example, on-processor block Jacobi iterations instead of a global inverse, or cycle-breaking on high-order curvilinear meshes,[22] it is straightforward to work out a reduced iteration similar to above, which stores φ and the degrees of freedom (DOF) of ψ_d necessary to update each direction d. Extending this to the Krylov setting takes a little more care but follows in an analogous manner.[23]

II.C. Heterogeneous DSA with Two Regions

Now, consider the case of heterogeneous domains, and suppose we partition the domain into thin and thick regions. In particular, let DOF/elements in which $\sigma_s(\mathbf{x}) < \eta$ be considered thin, denoted by subscript s, and let DOF/elements in which $\sigma_s(\mathbf{x}) \geq \eta$ be considered thick, denoted by subscript f. Then, order all matrices $\{\mathcal{L}_d\}$ in a block ordering:

$$\mathcal{L}_d = \begin{bmatrix} L_{ss} & L_{sf} \\ L_{fs} & L_{ff} \end{bmatrix} .$$

[c] Using $\Sigma \sim \sigma_s(\mathbf{x})$ is more common in literature; here, we use $\Sigma \sim \sigma_t(\mathbf{x})$ as derived in Ref. 6. In any case, they can be shown to have the same asymptotic efficiency in the thick limit.

Note that these regions do not have to be contiguous. Moving forward, subscripts d denoting angle are dropped on submatrices L_{ss}, L_{sf}, L_{fs}, and L_{ff}, for ease of notation. Note, however, that summations over direction d have an implied subscript on submatrices of $\mathcal{L}_d$.

Now, recall the two Schur complements of $\mathcal{L}_d$,

$$\begin{aligned} &\mathcal{S}_{ss} = L_{ss} - L_{sf}L_{ff}^{-1}L_{fs} \\ &\text{and} \\ &\mathcal{S}_{ff} = L_{ff} - L_{fs}L_{ss}^{-1}L_{sf} \ , \end{aligned} \tag{11}$$

and the closed form inverse of a 2×2 block matrix (see, for example, Sec. 3.2.11 in Ref. 24),

$$\mathcal{L}_d^{-1} = \begin{bmatrix} \mathcal{S}_{ss}^{-1} & -L_{ss}^{-1}L_{sf}\mathcal{S}_{ff}^{-1} \\ -\mathcal{S}_{ff}^{-1}L_{fs}L_{ss}^{-1} & \mathcal{S}_{ff}^{-1} \end{bmatrix} , \tag{12}$$

where

$$\begin{aligned} &\mathcal{S}_{ss}^{-1} = L_{ss}^{-1} + L_{ss}^{-1}L_{sf}\mathcal{S}_{ff}^{-1}L_{fs}L_{ss}^{-1} \\ &\text{and} \\ &\mathcal{S}_{ff}^{-1} = L_{ff}^{-1} + L_{ff}^{-1}L_{fs}\mathcal{S}_{ss}^{-1}L_{sf}L_{ff}^{-1} \end{aligned}$$

are interdependent expressions for the inverse of a Schur complement. Using Eq. (12), we can expand the Schur complement, Eq. (7), in block form as

$$\mathcal{S} = I - \sum_{d=1}^{n} \omega_d \mathcal{L}_d^{-1}\Sigma_s = I - \sum_{d=1}^{n} \omega_d \begin{bmatrix} \mathcal{S}_{ss}^{-1} & -L_{ss}^{-1}L_{sf}\mathcal{S}_{ff}^{-1} \\ -\mathcal{S}_{ff}^{-1}L_{fs}L_{ss}^{-1} & \mathcal{S}_{ff}^{-1} \end{bmatrix} \begin{bmatrix} \Sigma_{s,s} & \\ & \Sigma_{s,f} \end{bmatrix} . \tag{13}$$

Observe that Σ_s is a column scaling. Suppose the thin region is actually vacuum, in which case $\Sigma_{s,s} = \mathbf{0}$. Then,

$$\begin{aligned} \mathcal{S} &= I - \sum_{d=1}^{n} \omega_d \begin{bmatrix} \mathbf{0} & -L_{ss}^{-1}L_{sf}\mathcal{S}_{ff}^{-1}\Sigma_{s,f} \\ \mathbf{0} & \mathcal{S}_{ff}^{-1}\Sigma_{s,f} \end{bmatrix} \\ &= \begin{bmatrix} I & \sum_{d=1}^{n} \omega_d L_{ss}^{-1}L_{sf}\mathcal{S}_{ff}^{-1}\Sigma_{s,f} \\ \mathbf{0} & I - \sum_{d=1}^{n} \omega_d \mathcal{S}_{ff}^{-1}\Sigma_{s,f} \end{bmatrix} . \end{aligned} \tag{14}$$

Looking at Eq. (14), a natural choice of preconditioner for $\mathcal{S}$ is a block upper-triangular preconditioner, with blocks indicating thin and thick regions of the domain. Now, we only need to precondition the lower right (thick) block of Eq. (14), $I - \sum_{d=1}^{n} \omega_d \mathcal{S}_{ff}^{-1}\Sigma_{s,f}$. A natural choice here is to approximate $\mathcal{S}_{ff}^{-1}$ in the lower diagonal block (but not in the off-diagonal block) by L_{ff}^{-1}, in some sense a first-order approximation from Eq. (11). This yields

$$\mathcal{S} \approx \begin{bmatrix} I & \sum_{d=1}^{n} \omega_d L_{ss}^{-1}L_{sf}\mathcal{S}_{ff}^{-1}\Sigma_{s,f} \\ \mathbf{0} & I - \sum_{d=1}^{n} \omega_d L_{ff}^{-1}\Sigma_{s,f} \end{bmatrix} . \tag{15}$$

Now, disregarding boundary conditions, $I - \sum_{d=1}^{n} \omega_d L_{ff}^{-1}\Sigma_{s,f}$ corresponds to S_N transport only on the thick region, for which we know that diffusion is an effective preconditioning. Letting D_{ff}^{-1} denote an appropriate diffusion discretization over the thick region, we use the preconditioner $I + D_{ff}^{-1}\Sigma_{t,f} \approx (I - \sum_{d=1}^{n} \omega_d L_{ff}^{-1}\Sigma_{s,f})^{-1} \approx (I - \sum_{d=1}^{n} \omega_d \mathcal{S}_{ff}^{-1}\Sigma_{s,f})^{-1}$, which can be applied as the first step in a block upper-triangular preconditioning,

$$\begin{aligned} \mathcal{D}_T^{-1} &= \begin{bmatrix} I & \sum_{d=1}^{n} \omega_d L_{ss}^{-1}L_{sf}\mathcal{S}_{ff}^{-1}\Sigma_{s,f} \\ \mathbf{0} & (I + D_{ff}^{-1}\Sigma_{t,f})^{-1} \end{bmatrix}^{-1} \\ &= \begin{bmatrix} I & -\sum_{d=1}^{n} \omega_d L_{ss}^{-1}L_{sf}\mathcal{S}_{ff}^{-1}\Sigma_{s,f} \\ \mathbf{0} & I \end{bmatrix} \begin{bmatrix} I & \mathbf{0} \\ \mathbf{0} & I + D_{ff}^{-1}\Sigma_{t,f} \end{bmatrix} . \end{aligned} \tag{16}$$

The resulting preconditioning corresponds to a DSA preconditioning only on the thick region (including the interface), followed by using the updated thick solution as an additive correction to the thin region. Note that applying DSA only on the thick region is *not* the same as inverting a global diffusion operator and only updating the thick DOF.

To apply the additive correction in the left block of Eq. (16), following DSA on the thick region, note from Eq. (12) that

$$\begin{aligned} &\begin{bmatrix} I & -\sum_{d=1}^{n} \omega_d L_{ss}^{-1}L_{sf}\mathcal{S}_{ff}^{-1}\Sigma_{s,f} \\ \mathbf{0} & I \end{bmatrix} \\ &\quad = I + \begin{bmatrix} I & \mathbf{0} \\ \mathbf{0} & \mathbf{0} \end{bmatrix} \sum_{d=1}^{n} \omega_d \mathcal{L}_d^{-1}\Sigma_s \begin{bmatrix} \mathbf{0} & \mathbf{0} \\ \mathbf{0} & I \end{bmatrix} . \end{aligned}$$

This is nothing more than a modified transport update with zero right side. For all angles, the angular flux is first set to zero on the thin region, and then a transport

update is applied, inverting $\mathcal{L}_d$ for each direction d but only accumulating the solution corrections in thin DOF. The action of the preconditioner, Eq. (16), can be expressed as two steps in Algorithm 1.

Algorithm 1 (Triangular Heterogeneous DSA):

1. Let φ_f denote φ restricted to the thick region, and update $\varphi_f \leftarrow \varphi_f + D_{ff}^{-1}\Sigma_{t,f}\varphi_f$, where D_{ff} is a DSA diffusion preconditioner over the thick region.

2. Define $\overline{\varphi} := \begin{bmatrix} \mathbf{0} \\ \varphi_f \end{bmatrix}$, and let φ_s denote φ restricted to the thin region. For each direction d, update φ_s via

$$\varphi_s \leftarrow \varphi_s + \left[\omega_d \mathcal{L}_d^{-1}\Sigma_s\overline{\varphi}\right]_s.$$

In the case of $\Sigma_{s,s} = \mathbf{0}$, $\mathcal{S}$ is indeed block upper triangular, and the convergence of block-triangular preconditioned minimal-residual methods is defined by the approximation of the $(2,2)$ block in $\mathcal{S}$. For $\Sigma_{s,s} > 0$, $\mathcal{S}$ is no longer triangular, and convergence is then defined by preconditioning of the (2,2) Schur complement of $\mathcal{S}$ (Refs. 20). However, when $\Sigma_{s,s}$ is small, this preconditioning will likely be comparable to the preconditioning of the (2,2) block in $\mathcal{S}$, analogous to when $\Sigma_{s,s} = \mathbf{0}$. That is, convergence of heterogeneous DSA preconditioned source iteration is expected to be comparable for general $\Sigma_{s,s} \ll 1$, which is consistent with the numerical results in Sec. IV.

In many cases block-triangular preconditioners offer faster convergence than block-diagonal preconditioners, with marginal additional cost. For heterogeneous DSA, however, computing the action of the off-diagonal blocks requires a full parallel transport update. Thus, a second option for heterogeneous DSA preconditioning is a block-diagonal preconditioner, eliminating the need for the additional update in Algorithm 1. Define the following preconditioner:

$$\mathcal{D}_D^{-1} = \begin{bmatrix} I & \mathbf{0} \\ \mathbf{0} & I + D_{ff}^{-1}\Sigma_{t,f} \end{bmatrix} \tag{17}$$

for which the action can be described in Algorithm 2.

Algorithm 2 (Diagonal Heterogeneous DSA):

1. Let φ_f denote φ restricted to the thick region, and update $\varphi_f \leftarrow \varphi_f + D_{ff}^{-1}\Sigma_{t,f}\varphi_f$, where D_{ff} is the DSA diffusion preconditioner over the thick region.

When preconditioning by inverting the diagonal blocks of a 2×2 operator, block-diagonal preconditioned minimal-residual iterations generally converge to a given tolerance in roughly twice as many iterations as block-triangular preconditioners, due to not capturing off-diagonal coupling in the preconditioner.[20] For more general approximations (as used here), the difference in convergence between block-diagonal and block-triangular preconditioning is more complicated. In particular, there are situations where block-diagonal preconditioning can converge as fast as block-triangular preconditioning or can converge many times more slowly.[25] In almost all the problems we have tested, heterogeneous DSA appears to fall into the former: Block-diagonal preconditioning results in convergence as good as, or almost as good as, block-triangular preconditioning, at a fraction of the cost. Block-triangular preconditioning has resulted in fewer iterations on a few problems where $\Sigma_{s,s} \sim \mathcal{O}(1)$ is considered thin (for example, see Fig. 2 in Sec. IV.A.1), but because of the auxiliary update, the overall time to solution remained longer than with block-diagonal preconditioning. Block-diagonal preconditioning has the additional advantage over block-triangular preconditioning that it can be used with the conjugate gradient or minimum residual (MINRES) methods if the scalar flux problem is symmetrized, as in Refs. 26 and 27.

Thus, the main algorithm proposed here is very simple: Only apply DSA preconditioning on the thick region. It is immediately apparent why this is also compatible with voids, because if $\Sigma_t = \mathbf{0}$ on a certain region in the problem domain, a diffusion approximation (typically depending on Σ_t^{-1}) is neither formed nor inverted on that region. It is important to note that heterogeneous DSA is *not the same* as inverting a global DSA preconditioner and only applying updates to the thin region.

Remark 2 (Block-Diagonal Versus Block-Triangular Heterogeneous DSA): Examples were constructed in Ref. 25 where block-diagonal preconditioned minimal-residual iterations took up to $10\times$ more iterations to converge than with block-triangular preconditioning. If such a problem were to arise in transport, the auxiliary transport update in block-triangular heterogeneous DSA would likely be worth the added computational cost. Moreover, block-diagonal preconditioners typically rely more heavily on Krylov acceleration for convergence. When preconditioning source iteration without Krylov acceleration, block-triangular preconditioning likely provides a more robust method.

III. IMPLEMENTATION

III.A. DSA Discretizations

Conceptually, the heterogeneous preconditioning technique developed in Sec. II is flexible in terms of underlying transport and diffusion discretization. This paper focuses on DG discretizations of the spatial transport equation and thus, for consistency, DG DSA discretizations as well. Discontinuous Galerkin is of particular interest because the discontinuous finite element framework is amenable to traditional techniques such as sweeping and allows for high-order accuracy, including discretizing on high-order curvilinear finite elements.

A number of papers have considered DSA preconditioning for DG discretizations of S_N transport perhaps originally in Ref. 8 and more recently considering high-order discretizations in Refs. 6 and 16. Here, we build our DSA discretization based on the discrete analysis performed in Ref. 6 and extend modified stabilization ideas from Ref. 16. Following the standard derivation of DG discretization, the S_N transport equations in the diffusive-limit scaling[4] can be written in the discrete form

$$\begin{aligned}&\boldsymbol{\Omega}_d \cdot \mathbf{G}\psi^{(d)} + F^{(d)}\psi^{(d)} + \frac{1}{\varepsilon}\Sigma_t\psi^{(d)} \\ &\quad - \frac{1}{4\pi}\left(\frac{1}{\varepsilon}\Sigma_t - \varepsilon\Sigma_a\right)\varphi \\ &\quad = \frac{1}{4\pi}\left(\varepsilon\mathbf{q}_{inc}^{(d)} + \varepsilon\mathbf{q}^{(d)}\right),\end{aligned} \tag{18}$$

where

- ε = characteristic mean free path
- ψ_d = angular flux vector for the d'th discrete ordinates direction
- φ = scalar flux, given by $\varphi = \sum_d \omega_d \psi^{(d)}$, for quadrature weights $\{\omega_d\}$.

Right side vectors $q_{inc}^{(d)}$ and $q^{(d)}$ correspond to the linear forms

$$\begin{aligned}\left[q_{inc}^{(d)}\right]_m &= \sum_{\Gamma\in\mathcal{F}}\int_\Gamma \boldsymbol{\Omega}_d \cdot \mathbf{n} v_m \psi_{d,inc} dS \\ &\quad - \frac{1}{2}\sum_{\Gamma\in\mathcal{F}}\int_\Gamma |\boldsymbol{\Omega}_d \cdot \mathbf{n}| v_m \psi_{d,inc} dS\end{aligned}$$

and

$$\left[q^{(d)}\right]_m = \sum_\kappa \int_\kappa v_m q^{(d)} d\mathbf{x}$$

for finite element basis $\{v_m\}$. Here, Σ_a, Σ_s, and Σ_t are mass matrices corresponding to coefficients $\sigma_a(\mathbf{x})$, $\sigma_s(\mathbf{x})$, and $\sigma_t(\mathbf{x})$, respectively; $F^{(d)}$ is the DG face matrix based on upwinding with respect to $\boldsymbol{\Omega}_d$; and $\boldsymbol{\Omega}_d \cdot \mathbf{G}$ is the element-wise discretization of advection in direction $\boldsymbol{\Omega}_d$. For more details, see Ref. 6.

The analysis in Ref. 6 proves that a SIP discretization provides a robust DSA preconditioner in the optically thick limit, $\varepsilon \ll 1$, given by

$$\begin{aligned}D_{\text{SIP}} = &\frac{1}{\varepsilon}F_0 + \mathbf{G}^T \cdot \mathbf{I}\Sigma_t^{-1} \cdot \mathbf{G} + \mathbf{F}_1^T \cdot \Sigma_t^{-1}\mathbf{G} + \mathbf{G}^T \\ &\cdot \Sigma_t^{-1}\mathbf{F}_1 + \Sigma_a,\end{aligned} \tag{19}$$

where

$$F_0 = \frac{1}{4\pi}\sum_d w_d F_{[[]]}^{(d)}, \quad \mathbf{F}_1 = \frac{1}{4\pi}\sum_d w_d \boldsymbol{\Omega}_d F_{\{\}}^{(d)},$$
$$\mathbf{I} = \frac{1}{4\pi}\sum_d w_d \boldsymbol{\Omega}_d \boldsymbol{\Omega}_d,$$

and we perform discrete angular integration of the bilinear forms

$$\begin{aligned}\mathbf{v}^T F_{\{\}}^{(d)}\mathbf{u} &= -\sum_{\Gamma\in\mathcal{F}}\int_\Gamma \boldsymbol{\Omega}_d \cdot \mathbf{n}[\![u]\!]\{v\}dS, \quad \mathbf{v}^T F_{[[]]}^{(d)}\mathbf{u} \\ &= \sum_{\Gamma\in\mathcal{F}}\int_\Gamma \frac{1}{2}|\boldsymbol{\Omega}_d \cdot \mathbf{n}|[\![u]\!][\![v]\!]dS.\end{aligned}$$

Numerical results in Ref. 6 then indicate that dropping the face term $\mathbf{G}^T \cdot \Sigma_t^{-1}\mathbf{F}_1$, leading to a nonsymmetric interior penalty (NIP) discretization, provides a more robust preconditioner in non-optically thick material:

$$D_{\text{NIP}} = \frac{1}{\varepsilon}F_0 + \frac{1}{3}\mathbf{G}^T \cdot \Sigma_t^{-1}\mathbf{G} + \mathbf{F}_1^T \cdot \Sigma_t^{-1}\mathbf{G} + \Sigma_a. \tag{20}$$

For linear DG discretizations and straight-edged meshes, D_{NIP} is analogous to the Warsa-Wareing-Morel consistent diffusion discretization developed in Ref. 28. Moreover, with some work, one can show that D_{NIP} can also be derived by integrating the first two angular moments of Eq. (2). We use D_{NIP} as our baseline DSA discretization here, as we have found it to be far more robust on heterogeneous domains than D_{SIP}.

III.A.1. Modified Penalty Coefficient

The interior penalty term F_0 properly enforces continuity of the solution in Eqs. (19) and (20) in the

optically thick limit, $\varepsilon \ll 1$. However, the penalizing term scales as $\frac{1}{\varepsilon}F_0$ and tends to zero in the optically thin limit, $\varepsilon \gg 1$, and the preconditioners Eqs. (19) and (20) are found to be unstable. In particular, by continuity of eigenvalues as a function of matrix entries, as $\varepsilon \to 0$, Eq. (19) transitions continuously from being a symmetric positive definite operator to being an indefinite operator. This can lead to eigenvalues very close to zero, which are very difficult to precondition. We introduce the following modified penalizing term:

$$\tilde{F}_0 = \frac{1}{8\pi}\sum_d w_d \sum_\Gamma \int_\Gamma \max\left(\frac{c(p^{up})}{\sigma_t^{up} h^{up}}, 1\right) |\mathbf{\Omega}_d \cdot n| [\![u]\!][\![v]\!] dS. \tag{21}$$

where

n = normal vector to face Γ

h = cell size

$c(p) = Cp(p+1)$ for constant C (we use $C = 0.1$ via testing for the fastest convergence)

p = polynomial order of test and trial functions v and u

[[ ]] = jump operator

up = value on the upwind side at the integration point of face Γ with respect to direction $\mathbf{\Omega}_d$

and the sum is over mesh faces Γ.

Note that Eq. (21) coincides with the modified interior penalty formulation in Ref. 16, but it introduces a general formulation valid on curvilinear meshes, where the upwind value can vary along a highly curved face. The modified form of the penalty term Eq. (21) cancels the scaling ε^{-1} in the thin limit of Eqs. (19) and (20), and the penalization successfully enforces the continuity for any transport regime. mNIP is used to denote the resulting modified NIP discretization. Note that Eq. (21) is not compatible with regions of void, $\sigma_t = 0$. However, full DSA is incompatible with voids anyway, and as discussed in Sec. III.B, a nonmodified coefficient is most appropriate for heterogeneous preconditioning.

III.B. Heterogeneous DSA Implementation

Implementing heterogeneous DSA requires identifying and discretizing on a thick subdomain. In doing so, we want (a) the method to be amenable to easy addition to existing codes, (b) the DSA discretization to be an effective preconditioning on the thick subdomain, and (c) the DSA discretization on the subdomain to be solvable using standard AMG techniques.

Building on these ideas, we first define a tolerance η, where mesh elements such that $\sigma_s(\mathbf{x}) \geq \eta$ are considered thick and mesh elements such that $\sigma_s(\mathbf{x}) < \eta$ are considered thin. On every processor, it is straightforward to evaluate σ_s on each mesh element and track which elements are considered thick and thin. Next, suppose we discretize a global DSA operator (as if we are doing normal full DSA) and then extract the principal submatrix corresponding to thick DOF. The resulting matrix represents the thick region throughout the interior of the subdomain, with weakly enforced Dirichlet boundary conditions. If one writes carefully the stencil of heterogeneous NIP, it can be seen that the principal submatrix uses exclusively $\sigma_s(\mathbf{x}) \geq \eta$ corresponding to thick elements. On the other hand, heterogeneous mNIP introduces thin values $\sigma_s(\mathbf{x}) < \eta$ into the thick principal submatrix for all elements lying on the thick-thin boundary. This modification at the boundary makes for less robust preconditioning, which suggests (nonmodified) NIP as the appropriate heterogeneous discretization in practice.

The *hypre* library[7] now supports parallel extraction of submatrices from a parallel *hypre* matrix, given a (local) list of row/column indices. *hypre* is one of the standard parallel multigrid libraries and, if not already being used for linear solves in a software package, is easily connected to facilitate this operation.[d]

IV. NUMERICAL RESULTS

This section demonstrates the efficacy of the heterogeneous DSA approach on difficult problems in transport with heterogeneous cross sections. We emphasize both the superior and more robust preconditioning that heterogeneous DSA offers over traditional full DSA as well as the important property that the resulting linear systems are more tractable to solve, typically with $\mathcal{O}(1)$ AMG iterations, independent of problem size.

Algebraic multigrid solves are performed using BoomerAMG in the *hypre* library.[7] It is well known that the choice of parameters is important for AMG. Here, we use a V(1, 1) cycle with ℓ^1 hybrid Gauss-Seidel relaxation (*hypre* type 8) (Ref. 29), extended + i (distance-two)

[d] Note that for an optimized implementation, it is likely preferable to only discretize and construct the DSA matrix on the thick subdomain, particularly if the thick region is very small (for example, see Sec. IV.B). However, for many finite element libraries or existing code bases, this ends up being more intrusive to implement.

interpolation (*hypre* type 6) (Ref. 30), Hybrid Maximal Independent Set (HMIS) coarsening with one level of aggressive coarsening (*hypre* type 10) (Ref. 31), and a strength threshold of 0.05. These are similar parameters to the "optimized" parameters chosen for Parallel Deterministic Transport (PDT) runs in Ref. 32 with the important modification of using symmetric ℓ^1 hybrid Gauss-Seidel relaxation. In transport simulations, it is often the case that the spatial problem size per processor is relatively small, and ℓ^1 relaxation can be faster/more robust.[29] AMG is used as a preconditioner for the Generalized Minimal Residual (GMRES) method, which is solved to 10^{-4} relative residual tolerance.

Spatial linear transport equations are discretized using an upwind DG finite element method, constructed using the MFEM finite element library,[33] and an S_N discretization is used in angle. As discussed in Sec. II, the angular flux vectors are eliminated from the system, and only the scalar flux is stored and iterated on. Iterations are accelerated using fGMRES (Ref. 34), which is an important choice when using AMG-preconditioned Krylov methods to solve the DSA matrix because if the residual is not converged to very small tolerances, each iteration is actually a different preconditioner. It has been noted in multiple papers, originally in Refs. 5 and 26, that Krylov acceleration is important for heterogeneous domains. The same is true for the new heterogeneous DSA algorithm proposed here, and we do not present unaccelerated (fixed-point) results. The code does not have a traditional parallel sweeping implementation, but angular flux problems are solved using the nonsymmetric AMG method based on approximate ideal restriction[35,36] in the *hypre* library,[7] as studied in Ref. 37.

IV.A. The Crooked Pipe Problem

The first problem we consider is the so-called crooked pipe problem, originally introduced in Ref. 17 and discussed as a benchmark for DSA in Ref. 18. This is a steady-state test problem for thermal radiative transport with a single energy group and purely isotropic scattering throughout the domain. The domain is surrounded by vacuum, has a uniform isotropic radiation field, and has an inward isotropic source 10^4 times stronger than the radiation field. In Ref. 18 the problem is introduced with two scattering cross sections. Here, we modify the domain to have five regions, shown in Fig. 1, to allow for a larger variety of heterogeneities. Scattering cross section $\sigma_s(\mathbf{x})$ is defined to be piecewise constant over the subdomains shown in Fig. 1, and total cross section is then defined as $\sigma_t(\mathbf{x}) = \sigma_s(\mathbf{x}) + 1/cdt$, where c is the speed of light and dt is the time step of the transport solution. We use an S_8 angular discretization with 40 angles in the quadrature set (using the symmetry in two dimensions) and a second-order DG finite element discretization of the linear spatial transport equation for each angle unless otherwise noted.

IV.A.1. Two Cross Sections

To start, we consider only two cross sections,[17] one for the pipe (consistent with Fig. 1) and one for the wall, consisting of everything outside of the pipe (wall, edge, and block as denoted in Fig. 1). Consider the parameters used in Ref. 18:

$$\sigma_{pipe} = 200\,, \quad \sigma_{pipe} = 0.2\,, \quad cdt = 1000\,,$$

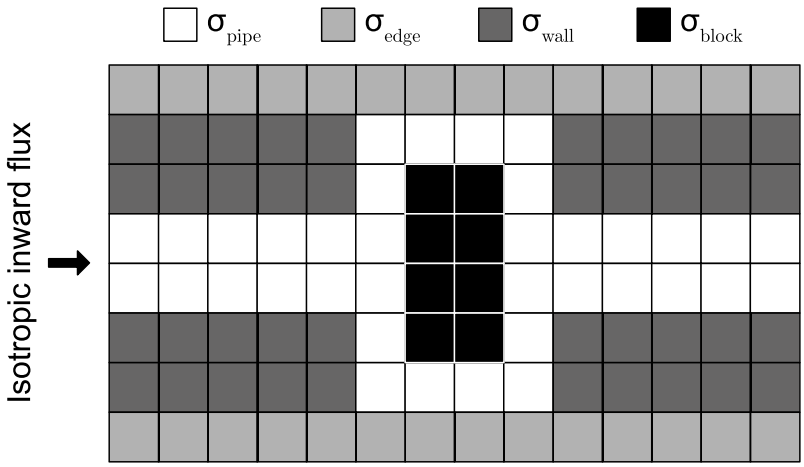

Fig. 1. A modification of the crooked pipe problem proposed in Ref. 18, here allowing for $\sigma_s(\mathbf{x})$ to have four different regions, denoted by varying shades from white to black. Each cell in the mesh is size 0.5×0.5.

where σ_{pipe} corresponds to all regions outside of the pipe. Because these are only moderately heterogeneous coefficients, we instead fix $\sigma_{pipe} = 200$ and $cdt = 1000$ as above and then scale σ_{pipe} from zero to 100 to test a wide range of heterogeneities. Numerical tests compare the newly developed heterogeneous DSA with full DSA, using NIP and mNIP DG diffusion discretizations (see Sec. III.A).

We start by applying heterogeneous DSA only to σ_{pipe} (that is, outside of the pipe), even for $\sigma_{pipe} \geq 1$, in order to determine what values of σ require DSA for good convergence. Figure 2a shows the number of fGMRES iterations to converge transport iterations to a relative residual tolerance of 10^{-12} [with DSA preconditioning applied directly using SuperLU (Ref. 38)], and Fig. 2b shows the number of AMG iterations to solve a representative DSA matrix to 10^{-12} relative residual.

There are a number of observations to note from Fig. 2:

1. Full DSA with NIP is robust across the entire range of σ_{pipe} (green right-pointing triangles, Fig. 2a); however, it is very difficult to solve for $\sigma_{pipe} \lessapprox 1$ (green right-pointing triangles, Fig. 2b), and we have tried many different variations of AMG and AMG-like techniques.

2. Full DSA with mNIP is solvable with AMG (black squares, Fig. 2b), but the preconditioned transport iteration requires about $5\times$ more iterations for convergence on the highly heterogeneous problems (black squares, Fig. 2a) compared with NIP preconditioning.

3. The results here are shown for heterogeneous DSA with NIP and mNIP. Recall from Sec. III.B that NIP provides a more natural boundary condition for heterogeneous preconditioning and will be used for most results. However, it should be noted that regions with small absorption $\sigma_a \ll 1$ and roughly $\sigma_s \in [1, 5]$ require preconditioning of the transport iteration, but wherein the NIP discretization can be difficult to solve using AMG. Here, we demonstrate that mNIP may be an effective option as well, although the heterogeneous preconditioning would be less robust in theory (and, in our experience, also less robust in practice).

4. Heterogeneous DSA is applied *only outside of the pipe* for these tests, even when the pipe is moderately thick. As expected, convergence of heterogeneous DSA deteriorates rapidly when σ_{pipe} is not thin, as such regimes are known to require preconditioning. In practice, there is a switch so that DSA can be applied to all regions such that $\sigma_s(\mathbf{x}) \geq \eta$ for some tolerance η. If $\sigma_{pipe} > \eta$ for all $\mathbf{x}$, heterogeneous DSA breaks down to traditional DSA. Figure 2 suggests a tolerance of $\eta \approx 1.0$ to minimize the total number of iterations, while ensuring heterogeneous NIP DSA is solvable with AMG. Note here that we have small absorption, $\sigma_a \sim 1/cdt = 10^{-3}$, and see comparable results down to zero absorption (e.g., see later results in Table II). For regions with large absorption, a larger η may be possible (resulting in a smaller thick subdomain), but it is also likely unnecessary; that is, $\eta \approx 1$ will provide effective preconditioning.

5. For $\sigma_{pipe} < 0.1$, heterogeneous DSA with NIP yields identical iteration counts as full DSA with NIP and up to a $5\times$ reduction in iterations compared to DSA with mNIP. Moreover, AMG solvers are robust when applied to

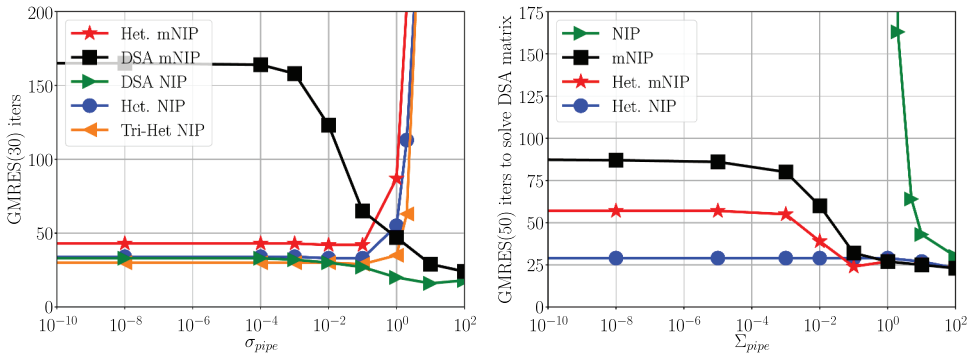

(a) (b)

Fig. 2. Results related to DSA preconditioners applied to the crooked pipe problem with $\sigma_{pipe} = 200$ and $cdt = 1000$, where heterogeneous DSA is only applied outside of the pipe. (a) Comparison of fGMRES transport iterations to 10_{-12} relative residual tolerance for various DSA and heterogeneous DSA preconditioners as a function of σ_{pipe}. DSA matrices are inverted directly. (b) Total number of GMRES iterations, preconditioned by AMG, to solve the DSA matrix to a relative residual tolerance of 10_{-12}, for a single transport iteration. Note that the results in (a) and (b) are independent, separately demonstrating convergence of transport iterations and AMG.

heterogeneous DSA, only requiring 20 to 28 iterations to obtain 12 digits of accuracy (blue circles and red stars, Fig. 2b).

6. Triangular heterogeneous DSA only offers a significant reduction in iteration count over diagonal heterogeneous DSA for a small range of $\sigma_{pipe} \in [1, 5]$. At best, triangular heterogeneous DSA requires $1.8\times$ fewer iterations than diagonal heterogeneous DSA for $\sigma_{pipe} = 5$ but with a likely comparable added computational cost of an additional sweep each iteration. Thus,

TABLE I

Coefficients $\sigma_s(\mathbf{x})$ for Five Test Problems

Problem Number	Parameters				Thin/Thick	
	σ_{pipe}	σ_{wall}	σ_{edge}	σ_{block}	Percent Thin	Percent Thick
1	1e-3	500	1e-4	100	55%	45%
2	0.1	200	200	5	32%	68%
3	1e-4	10	500	0.1	39%	61%
4	1e-6	0.1	100	1000	68%	32%
5	1e-4	10	500	100	32%	68%

TABLE II

DSA-Preconditioned GMRES(30) Iterations to 10^{-12} Relative Residual for Problems 1 through 5, with an S_8 Angular Discretization and Second-Order or Fourth-Order DG Spatial Discretization

Row	Parameters			Full DSA		Heterogeneous DSA
	Problem Number	*cdt*	Order	NIP	mNIP	NIP
1	1	1	2	19	56	15
2	2	1	2	18	41	15
3	3	1	2	16	41	13
4	4	1	2	19	58	15
5	5	1	2	20	44	15
6	1	10^3	2	31	120	25
7	2	10^3	2	25	61	25
8	3	10^3	2	23	96	20
9	4	10^3	2	26	132	22
10	5	10^3	2	102	143	25
11	1	10^8	2	34	123	25
12	2	10^8	2	25	64	25
13	3	10^8	2	28	98	21
14	4	10^8	2	116	134	22
15	5	10^8	2	134	147	25
16	1	$\sigma_a = 0$	2	34	153	25
17	2	$\sigma_a = 0$	2	25	94	25
18	3	$\sigma_a = 0$	2	24	128	21
19	4	$\sigma_a = 0$	2	119	164	22
20	5	$\sigma_a = 0$	2	DNC[a]	177	25
21	1	$\sigma_a = 0$	4	42	79	25
22	2	$\sigma_a = 0$	4	59	40	36
23	3	$\sigma_a = 0$	4	59	57	21
24	4	$\sigma_a = 0$	4	59	73	22
25	5	$\sigma_a = 0$	4	DNC	70	27

[a]DNC denotes did not converge in 500 iterations.

it seems unlikely the triangular version will be a better choice in practice, consistent with the discussion in Sec. II.C.

Based on these results, let the tolerance $\eta = 1$ moving forward. The following sections consider harder problems using full DSA with NIP and mNIP and diagonal heterogeneous DSA with NIP.

IV.A.2. Multiple Cross Sections

Above, we took a benchmark problem and demonstrated the robustness and benefits of heterogeneous DSA. In this section, we take the same problem but use the full five regions of cross section indicated in Fig. 1 to allow for a wider variety of heterogeneities and (hypothetically) more difficult problems. Table I provides five different sets of scattering cross sections $\sigma_s(\mathbf{x})$ in the five subregions in Fig. 1. Letting $\eta = 1$ distinguish between thick and thin regions, the percentage of the domain for each is also given.

Results using 32 cores and ≈ 2500 to 5000 DOF/core are shown in Table II. Tests are run for $cdt = 1, 1000,$ and 10^8, as well as the limiting case of zero absorption, $\sigma_a = 0$, and for second-order and fourth-order finite elements. All DSA matrices are inverted directly using SuperLU (Ref. 38) in order to compare the preconditioning of S_N transport, independent of the solvability of the DSA matrix.

Note that the heterogeneous DSA method with NIP is as good as or better than standard DSA with NIP or mNIP in all cases. For some problems, heterogeneous DSA takes 5 to 6× fewer iterations (see rows 14/15 and 19 in Table II) than full DSA or converges when full DSA with NIP does not (see rows 20 and 25 in Table II). The lack of convergence of DSA with NIP in rows 20 and 25 is likely due to a (near-)singular NIP DSA matrix that cannot be accurately inverted even with a direct solver.

Next, we consider a refined spatial mesh, with an S_8 angular discretization and second-order DG finite elements (≈ 1 million spatial DOF), and look at convergence of DSA preconditioned with NIP, mNIP, and heterogeneous NIP. All simulations are run on 256 cores, and DSA solves are performed using a maximum of 250 AMG iterations. In Table III, we see that full DSA with NIP does not converge for $cdt \gg 1$, largely because 250 AMG iterations provide a very poor approximation to the diffusion inverse. On the refined mesh, mNIP iterations to convergence actually decrease (compared with Table II), and each iteration requires only a modest

TABLE III

DSA-Preconditioned fGMRES(30) Iterations to 10^{-12} Relative Residual and AMG-Preconditioned GMRES Iterations to Apply a Single DSA Preconditioning to 10^{-4} Relative Residual

Parameters		DSA NIP		DSA mNIP		Heterogeneous DSA NIP	
Problem Number	*cdt*	Iters.[a]	AMG it.[b]	Iters.	AMG it.	Iters.	AMG it.
1	1	35	DNC[c]	39	14	15	7
2	1	27	DNC	23	8	17	45
3	1	34	DNC	29	10	13	29
4	1	38	DNC	42	10	13	9
5	1	37	DNC	30	10	14	30
1	10^3	DNC	DNC	73	99	25	9
2	10^3	DNC	DNC	40	13	29	180
3	10^3	DNC	DNC	55	33	22	36
4	10^3	DNC	DNC	71	26	23	12
5	10^3	DNC	DNC	78	34	27	35
1	10^8	DNC	DNC	71	145	25	9
2	10^8	DNC	DNC	40	12	29	180
3	10^8	DNC	DNC	55	42	22	36
4	10^8	DNC	DNC	73	43	23	12
5	10^8	DNC	DNC	75	41	27	35

[a]Iters. denotes DSA-preconditioned fGMRES(30) iterations to 10^{-12} relative residual.
[b]AMG it. denotes AMG-preconditioned GMRES iterations to apply a single DSA preconditioning to 10^{-4} relative residual.
[c]DNC denotes did not converge in 500 iterations.

number of AMG iterations. However, heterogeneous NIP provides faster convergence for the transport iterations in all cases, typically yielding a 2 to 3× reduction in iteration count, for comparable (sometimes less, sometimes more) AMG iterations.

It should be noted that AMG struggles on the heterogeneous preconditioning for problem 2. Interestingly, this is also the easiest problem for full DSA with mNIP. These are related and are because (a) problem 2 does not have any particularly thin regions or particularly big discontinuities in σ (see Table I), where full DSA with mNIP is least effective (see Fig. 2a), and (b) problem 2 has a region of $\sigma = 5$. Cross sections $\sigma_s \sim \mathcal{O}(1)$ (with small σ_a) are exactly the interface where DSA preconditioning is necessary for good convergence of source iteration, but AMG applied to (nonmodified) DG discretizations begins to struggle (see Fig. 2). It should be noted that applying mNIP with heterogeneous DSA yields a comparable iteration count to full DSA in terms of both AMG and source iteration. We do not include these results because for all other tested problems, heterogeneous DSA with mNIP yields a significant increase in outer transport iteration count over heterogeneous DSA with NIP, with only a marginal reduction in AMG iterations. However, we do note that heterogeneous DSA is best suited for problems with large regions of $\sigma_s \ll 1$ and/or $\sigma_s \gg 1$.

IV.B. Hohlraum

The second problem we consider represents a realistic setting of the hohlraum chamber with a fuel capsule. This design is used in the indirect-drive approach of ICF. Radiation transport plays a fundamental role in the indirect-drive scenario, where the gold wall of the hohlraum, heated by lasers to a high temperature, radiates X-rays that propagate through a low-density helium fill. This causes a compression of the fuel capsule as the photons are absorbed on its surface. The capsule is filled with hydrogen, contained inside a thin layer of plastic (CH) on its surface, with a small hole on the right simulating a filling tube. The cross section and emissivity of a material are strongly dependent on its composition and temperature, making X-ray radiation transport a highly nonlinear process.

This can be represented by a time-dependent thermal radiative transfer problem modeled by a transport equation with a pseudo-scattering term[39,40] σ_{ps} and a corresponding source of gray-body radiation q_{ps}, both as a function of coefficient σ:

$$\sigma_{ps} = \frac{\sigma^2 16\pi acT^3}{\frac{C_v}{\Delta t} + 16\pi\sigma acT^3} \tag{22}$$

and

$$q_{ps} = \sigma_a acT^4 - \frac{\sigma^2 16\pi a^2 c^2 T^7}{\frac{C_v}{\Delta t} + 16\pi\sigma acT^3}, \tag{23}$$

where

T = plasma temperature
C_v = heat capacity

$$c = 2.9979 \times 10^4$$

$$a = 137.199 = \text{radiation constant}$$

and we use a very long time step $\Delta t = 10^{-3}$ μs, corresponding to $\approx 10\%$ of the duration of a common ICF simulation. The unit system of the National Ignition Facility is used.[41] The hohlraum problem introduces four different materials: gold (blue), helium (red), CH (green), and hydrogen (yellow), each with a different cross section and heat capacity as shown in Fig. 3a, and with corresponding σ and C_v values given in Table IV.

Here, we consider a steady-state test of a single time step, modeled by Eq. (2) with a single energy group, and purely isotropic scattering throughout the domain. In the notation of Eq. (2), we have $\sigma_s(\mathbf{x}) = \sigma_{ps}(\mathbf{x})$ and $\sigma_t(\mathbf{x}) = \sigma(\mathbf{x})$, with the radiation source as $q_d(\mathbf{x}) = q_{ps}(\mathbf{x})$. The domain is surrounded by vacuum and has an initially uniform temperature $T = 10^{-3}$ keV, and the source q_{ps} on the hohlraum gold wall corresponds to $T = 0.4$ keV. The solution of the scalar flux radiation field produced by a laser-heated gold wall is shown in Fig. 3b. In large-scale problems the pseudo-scattering equation is solved iteratively, and standard iterative methods converge very slowly when either the time step or σ is large. Extreme heterogeneities are encountered in such cases, in particular, on the gold-helium and CH-helium material interfaces.

Table V shows results for DSA and heterogeneous DSA preconditioning of a fourth-order DG discretization in space, and S_4, S_8, and S_{12} angular discretizations. Simulations are run on 16, 64, and 256 cores, corresponding to the three levels of refinement shown, with ≈ 5000 spatial DOF/core. Performance of AMG on the hohlraum problem is particularly poor for full DSA. Results for full DSA with NIP are not shown in Table III because AMG iterations make no significant

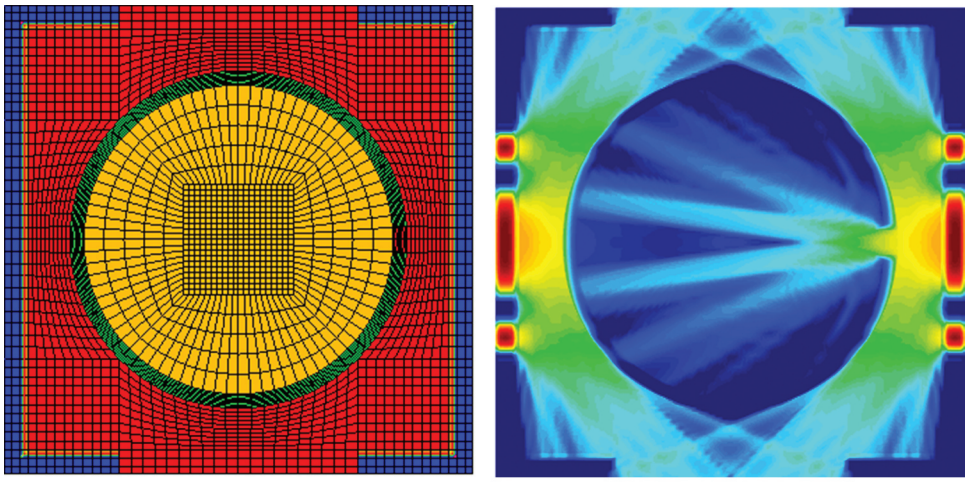

Fig. 3. Indirect-drive ICF approach using a gold cylindrical chamber (hohlraum) filled with helium and a fuel capsule placed in the middle. (a) Hohlraum mesh, with materials represented as colors: gold ↔ blue, helium ↔ red, CH ↔ green, and hydrogen ↔ yellow (left–to–right: blue, red, green, yellow, green, red, blue). (b) Scalar flux solution (S_{18}) due to radiation source from the laser–heated gold wall (red regions ~ laser heating).

TABLE IV

Opacities $\sigma_a(\mathbf{x})$ and Heat Capacities $C_v(\mathbf{x})$ for Given Materials

	Hohlraum Gold Wall	Helium Fill	Capsule CH Layer	Capsule Hydrogen Fuel
σ	10^3	10^{-3}	10^2	1
C_v	10^5	10^{-2}	10^3	1

TABLE V

DSA-Preconditioned fGMRES Iterations to 10^{-12} Relative Residual, AMG-Preconditioned fGMRES Iterations to 10^{-4} Relative Residual Tolerance (with a Maximum 250 AMG Iterations), and Percentage of DOF Marked "Thick," for the Hohlraum Problem

		DSA mNIP		Heterogeneous DSA NIP		
S_N	DOF	Iters.[a]	AMG it.[b]	Iters.	AMG it.	Percent Thick DOF
4	78 900	52	DNC[c]	20	6	2.3%
4	315 600	40	DNC	23	8	2.9%
4	1 262 400	28	DNC	20	10	2.5%
8	78 900	52	DNC	20	6	2.3%
8	315 600	40	DNC	23	7	2.9%
8	1 262 400	29	DNC	21	10	2.5%
12	78 900	52	DNC	20	6	2.3%
12	315 600	39	DNC	23	7	2.9%
12	1 262 400	29	DNC	21	10	2.5%

[a]Iters. denotes DSA-preconditioned fGMRES(30) iterations to 10^{-12} relative residual.
[b]AMG it. denotes AMG-preconditioned GMRES iterations to apply a single DSA preconditioning to 10^{-4} relative residual.
[c]DNC denotes did not converge in 500 iterations.

reduction in residual for the DSA solve, and thus, the larger transport iterations do not converge. AMG is also unable to solve the full DSA with mNIP matrices (1000 AMG-preconditioned GMRES iterations reduced the residual less than two orders of magnitude), but apparently enough preconditioning is achieved in 250 iterations for the larger transport iterations to achieve reasonable convergence. However, we would not consider this a robust method, as results for full DSA with NIP here and in Table III indicate that if the AMG iterations are ineffective, the preconditioning may also be ineffective, and the transport iterations may not converge. Moreover, it is likely AMG convergence will continue to degrade as the spatial problem is further refined, which may eventually prevent convergence of the larger transport iterations. Note that we also tried multiple scaling constants for mNIP and saw no notable improvement in AMG convergence.

In contrast, heterogeneous DSA proves to be fast and robust. Heterogeneous DSA converges in fewer iterations than full DSA for all tested problem sizes and S_N orders, reducing total iteration counts between 30% to more than 2.5 × for the coarsest mesh. Moreover, AMG proves effective as a solver for heterogeneous NIP, requiring at most ten AMG iterations to reduce the residual four orders of magnitude. This highlights how interesting the dynamics of the problem and preconditioning can be: Without DSA preconditioning, source iteration on this problem converges extremely slowly. Preconditioning a very small subdomain (less than 3% of the mesh elements!) with ten AMG iterations results in rapid convergence, independent of spatial mesh refinement or S_N order.

V. CONCLUSIONS

This paper introduces a new DSA-like technique to precondition transport iteration in highly heterogeneous domains, which is trivially compatible with voids. The preconditioning is based on a linear algebraic analysis rather than the underlying physics but proves to be at least as fast as standard full DSA on all problems we tested and reduces the iteration count by 5 to 6× on some examples. Moreover, even for robust DSA discretizations based on integrating angular moments, the resulting linear systems are typically solvable using $\mathcal{O}(1)$ AMG iterations, while the same discretization applied to the entire domain (full DSA) can lead to matrices that are very difficult or intractable to solve.

Even with optimized AMG parameters and a state-of-the-art parallel AMG library, the application of DSA can take a remarkably large portion of the solve phase for S_N transport, as high as 60% with a small number of mesh elements per core.[32] For difficult problems like the hohlraum discussed in Sec. IV.B, AMG simply does not converge, and it is unclear if the preconditioned transport iterations will converge. In addition to making the DSA solves tractable, only having to solve a DSA discretization on the moderately thick to thick subdomains can also significantly reduce the percentage of time the DSA solves take. The hohlraum problem studied in Sec. IV.B only requires DSA preconditioning on less than 3% of the mesh elements for rapid convergence. Finally, the proposed approach is relatively nonintrusive and easy to add to existing high-performance transport codes.

Numerical results in Sec. IV indicate rather different behavior on different heterogeneous configurations of σ_t, in terms of DSA preconditioning and AMG convergence. Analyzing this problem is nontrivial as it is based on an approximation to a sum of Schur complement inverses, Eq. (15). A unified framework for DSA preconditioning, including the heterogeneous approach developed here, as well as a better understanding of how discretization properties and parameters affect both DSA preconditioning and the performance of multigrid-like solvers remains an outstanding issue and long-term objective.

Acknowledgments

This material is based upon work supported by the U.S. Department of Energy, National Nuclear Security Administration, under award number DE-NA0002376. This work was performed under the auspices of the U.S. Department of Energy by Lawrence Livermore National Laboratory under contract DE-AC52-07NA27344 (LLNL-JRNL-802400).

ORCID

B. S. Southworth http://orcid.org/0000-0002-0283-4928
Milan Holec http://orcid.org/0000-0001-7016-0729
T. S. Haut http://orcid.org/0000-0001-6505-1472

References

1. H. J. KOPP, "Synthetic Method Solution of the Transport Equation," *Nucl. Sci. Eng.*, **17**, *1*, 65 (1963); https://doi.org/10.13182/NSE63-1.
2. V. I. LEBEDEV, "The Iterative kp Method for the Kinetic Equation," *Proc. Conf. Mathematical Methods for Solving Nuclear Physics Problems*, Dubna, Russia, 1964, p. 17 (1964).
3. R. E. ALCOUFFE, "Diffusion Synthetic Acceleration Methods for the Diamond-Differenced Discrete-Ordinates

Equations," *Nucl. Sci. Eng.*, **64**, *2*, 344 (1977); https://doi.org/10.13182/NSE77-1.

4. E. W. LARSEN, "Unconditionally Stable Diffusion-Synthetic Acceleration Methods for the Slab Geometry Discrete Ordinates Equations. Part 1: Theory," *Nucl. Sci. Eng.*, **82**, *1*, 47 (1982); https://doi.org/10.13182/NSE82-1.

5. J. S. WARSA, T. A. WAREING, and J. E. MOREL, "Krylov Iterative Methods and the Degraded Effectiveness of Diffusion Synthetic Acceleration for Multidimensional S_N Calculations in Problems with Material Discontinuities," *Nucl. Sci. Eng.*, **147**, *3*, 218 (July 2004); https://doi.org/10.13182/NSE02-14.

6. T. S. HAUT et al., "Diffusion synthetic acceleration preconditioning for discontinuous Galerkin discretizations of S_N transport on high-order curved meshes," *SIAM J. Sci. Comput.* (Oct. 2018) (submitted for publication). doi.org/10.1137/19M124993X.

7. R. D. FALGOUT and U. M. YANG, "*hypre*: A Library of High Performance Preconditioners," *Proc. Int. Conf. Computational Science (ICCS 2002) [Lecture Notes in Computer Science 2331]*, Amsterdam, Netherlands, April 21–24, 2002, p. 632 (2002); https://link.springer.com/content/pdf/10.1007%2F3-540-47789-6_66.pdf (current as of Feb. 3, 2020).

8. J. S. WARSA et al., "Two-Level Preconditioning of a Discontinuous Galerkin Method for Radiation Diffusion," *Numerical Mathematics and Advanced Applications*, p. 967, Springer Verlag Italia, Milan, Italy (2003).

9. B. O'MALLEY et al., "Hybrid Multi-Level Solvers for Discontinuous Galerkin Finite Element Discrete Ordinate Diffusion Synthetic Acceleration of Radiation Transport Algorithms," *Ann. Nucl. Energy*, **102**, 134 (Apr. 2017); https://doi.org/10.1016/j.anucene.2016.11.048.

10. L. N. OLSON and J. B. SCHRODER, "Smoothed Aggregation Multigrid Solvers for High-Order Discontinuous Galerkin Methods for Elliptic Problems," *J. Comput. Phys.*, **230**, *1*, 6959 (Aug. 2011); https://doi.org/10.1016/j.jcp.2011.05.009.

11. P. BASTIAN, M. BLATT, and R. SCHEICHL, "Algebraic Multigrid for Discontinuous Galerkin Discretizations of Heterogeneous Elliptic Problems," *Numer. Linear Algebra Appl.*, **19**, *2*, 367 (Feb. 2012); https://doi.org/10.1002/nla.1816.

12. P. F. ANTONIETTI et al., "A Uniform Additive Schwarz Preconditioner for High-Order Discontinuous Galerkin Approximations of Elliptic Problems," *J. Sci. Comput.*, **70**, *2*, 608 (Aug. 2016); https://doi.org/10.1007/s10915-016-0259-9.

13. Y. WANG, H. ZHANG, and R. C. MARTINEAU, "Diffusion Acceleration Schemes for Self-Adjoint Angular Flux Formulation with a Void Treatment," *Nucl. Sci. Eng.*, **176**, *2*, 201 (Mar. 2017); https://doi.org/10.13182/NSE12-83.

14. H. R. HAMMER, J. E. MOREL, and Y. WANG, "Nonlinear Diffusion Acceleration of the Least-Squares Transport Equation in Geometries with Voids," *Nucl. Sci. Eng.*, **193**, *5*, 453 (Jan. 2019); https://doi.org/10.1080/00295639.2018.1542865.

15. S. YE, H. AN, and X. XU., "A Local Character Based Method for Solving Linear Systems of Radiation Diffusion Problems," *J. Comput. Phys.*, **407**, 109218 (2020); https://doi.org/10.1016/j.jcp.2019.109218.

16. Y. WANG and J. C. RAGUSA, "Diffusion Synthetic Acceleration for High-Order Discontinuous Finite Element S_N Transport Schemes and Application to Locally Refined Unstructured Meshes," *Nucl. Sci. Eng.*, **166**, *2*, 145 (Oct. 2010); https://doi.org/10.13182/NSE09-46.

17. N. A. GENTILE, "Implicit Monte Carlo Diffusion—An Acceleration Method for Monte Carlo Time-Dependent Radiative Transfer Simulations," *J. Comput. Phys.*, **172**, *2*, 543 (2001); https://doi.org/10.1006/jcph.2001.6836.

18. R. P. SMEDLEY-STEVENSON, A. W. HAGUES, and J. KÓPHÁZI, "A Benchmark for Assessing the Effectivenesss of Diffusion Synthetic Acceleration Schemes," *Proc. Int. Conf. Mathematics and Computation (M&C), Supercomputing in Nuclear Applications (SNA) and Monte Carlo (MC) (M&C+SNA+MC 2015)*, Nashville, Tennessee, April 19–23, 2015, American Nuclear Society (2015).

19. V. FABER and T. A. MANTEUFFEL, "A Look at Transport Theory from the Point of View of Linear Algebra," *Proc. Conf. Transport Theory, Invariant Imbedding, and Integral Equations*, Santa Fe, New Mexico, January 1988, p. 37, Dekker (1989).

20. B. S. SOUTHWORTH, A. A. SIVAS, and S. RHEBERGEN, "On Fixed-Point, Krylov, and Block Preconditioners for Nonsymmetric Problems," *SIAM Journal on Matrix Analysis and Applications*, **41**, *871 (2020); https://doi.org/10.1137/19M1298317.*

21. J. S. WARSA, K. THOMPSON, and J. E. MOREL, "Improving the Efficiency of Simple Parallel S_N Algorithms with Krylov Iterative Methods," *Trans. Am. Nucl. Soc.*, **89**, 449 (2003).

22. T. S. HAUT et al., "An Efficient Sweep-Based Solver for the S_N Equations on High-Order Meshes," *Nucl. Sci. Eng.*, **193**, 746 (2019).

23. Y. WANG, "Adaptive Mesh Refinement Solution Techniques for the Multigroup SN Transport Equation Using a Higher-Order Discontinuous Finite Element Method," Texas A&M University (2009).

24. G. H. GOLUB and C. F. VAN LOAN, *Matrix Computations*, 4th ed., The Johns Hopkins University Press, Baltimore, Maryland (2013).

25. B. S. SOUTHWORTH and S. S. OLIVIER, "A Note on 2×2 Block-Diagonal Preconditioning," arXiv preprint arxiv:2001.00711 (2019).

26. A. GUPTA and R. S. MODAK, "On the Use of the Conjugate Gradient Method for the Solution of the Neutron Transport Equation," *Ann. Nucl. Energy*, **29**, *16*, 1933 (Nov. 2002); https://doi.org/10.1016/S0306-4549(02)00017-8.

27. B. CHANG, "The Conjugate Gradient Method Solves the Neutron Transport Equation H-Optimally," *Numer. Linear Algebra Appl.*, **14**, *10*, 751 (Dec. 2007); https://doi.org/10.1002/nla.551.

28. J. S. WARSA, T. A. WAREING, and J. E. MOREL, "Fully Consistent Diffusion Synthetic Acceleration of Linear Discontinuous S_N Transport Discretizations on Unstructured Tetrahedral Meshes," *Nucl. Sci. Eng.*, **141**, *3*, 236 (2002); https://doi.org/10.13182/NSE141-236.

29. A. H. BAKER et al., "Multigrid Smoothers for Ultraparallel Computing," *SIAM J. Sci. Comput.*, **33**, *5*, 2864 (2011); https://doi.org/10.1137/100798806.

30. H. DE STERCK et al., "Distance-Two Interpolation for Parallel Algebraic Multigrid," *Numer. Linear Algebra Appl.*, **15**, *2–3*, 115 (2008); https://doi.org/10.1002/nla.559.

31. H. DE STERCK, U. M. YANG, and J. J. HEYS, "Reducing Complexity in Parallel Algebraic Multigrid Preconditioners," *SIAM J. Matrix Anal. Appl.*, **27**, *4*, 1019 (Jan. 2006); https://doi.org/10.1137/040615729.

32. M. HANUS, "Weak Scaling of DSA Preconditioning of Transport Sweeps Using HYPRE," arXiv preprint arXiv:1911.04624 (2019).

33. V. A. DOBREV et al., "MFEM: Modular Finite Element Methods," MFEM website; http://mfem.org (2018) (current as of Feb. 3, 2020).

34. Y. SAAD, "A Flexible Inner-Outer Preconditioned GMRES Algorithm," *SIAM J. Sci. Comput.*, **14**, *2*, 461 (Mar. 1993); https://doi.org/10.1137/0914028.

35. T. A. MANTEUFFEL, J. W. RUGE, and B. S. SOUTHWORTH, "Nonsymmetric Algebraic Multigrid Based on Local Approximate Ideal Restriction (ℓAIR)," *SIAM J. Sci. Comput.*, **40**, *6*, A4105 (Dec. 2018); https://doi.org/10.1137/17M1144350.

36. T. A. MANTEUFFEL et al., "Nonsymmetric Reduction-Based Algebraic Multigrid," *SIAM J. Sci. Comput.*, **41**, *5*, S242 (2019); https://doi.org/10.1137/18M1193761.

37. J. HANOPHY et al., "Parallel Approximate Ideal Restriction Multigrid for Solving the S_N Transport Equations," *Nucl. Sci. Eng.* (2020); https://doi.org/10.1080/00295639.2020.1747263.

38. X. S. LI et al., "Superlu Users' Guide," Lawrence Berkeley National Laboratory (1999).

39. J. A. FLECK and J. D. CUMMINGS, "An Implicit Monte Carlo Scheme for Calculating Time and Frequency Dependent Nonlinear Radiation Transport," *J. Comput. Phys.*, **8**, *3*, 313 (1971); https://doi.org/10.1016/0021-9991(71)90015-5.

40. E. W. LARSEN, "A Grey Transport Acceleration Method for Time-Dependent Radiative Transfer Problems," *J. Comput. Phys.*, **78**, *2*, 459 (1988); https://doi.org/10.1016/0021-9991(88)90060-5.

41. M. M. MARINAK et al., "Advances in Hydra and Its Application to Simulations of Inertial Confinement Fusion Targets," *EPJ Web Conf.*, **59**, 01 (2008).